



Fermi National Accelerator Laboratory

FERMILAB-Pub-92/380-E

Measurement of the Cross Section for Production of Two Isolated Prompt Photons in $\bar{p}p$ Collisions at $\sqrt{s} = 1.8$ TeV

F. Abe et al
The CDF Collaboration

*Fermi National Accelerator Laboratory
P.O. Box 500, Batavia, Illinois 60510*

December 1992

Submitted to *Physical Review Letters*

Disclaimer

This report was prepared as an account of work sponsored by an agency of the United States Government. Neither the United States Government nor any agency thereof, nor any of their employees, makes any warranty, express or implied, or assumes any legal liability or responsibility for the accuracy, completeness, or usefulness of any information, apparatus, product, or process disclosed, or represents that its use would not infringe privately owned rights. Reference herein to any specific commercial product, process, or service by trade name, trademark, manufacturer, or otherwise, does not necessarily constitute or imply its endorsement, recommendation, or favoring by the United States Government or any agency thereof. The views and opinions of authors expressed herein do not necessarily state or reflect those of the United States Government or any agency thereof.

Measurement of the Cross Section for Production of Two Isolated Prompt Photons in $\bar{p}p$ Collisions at $\sqrt{s} = 1.8$ TeV

F. Abe,⁽¹¹⁾ M. Albrow,⁽⁶⁾ D. Amidei,⁽¹⁴⁾ C. Anway-Wiese,⁽³⁾ G. Apollinari,⁽²⁰⁾
M. Atac,⁽⁶⁾ P. Auchincloss,⁽¹⁹⁾ P. Azzi,⁽¹⁵⁾ A. R. Baden,⁽⁸⁾ N. Bacchetta,⁽¹⁵⁾
W. Badgett,⁽¹⁴⁾ M. W. Bailey,⁽¹⁸⁾ A. Bamberger,^(6,a) P. de Barbaro,⁽¹⁹⁾ A. Barbaro-
Galtieri,⁽¹²⁾ V. E. Barnes,⁽¹⁸⁾ B. A. Barnett,⁽¹⁰⁾ G. Bauer,⁽¹³⁾ T. Baumann,⁽⁸⁾
F. Bedeschi,⁽¹⁷⁾ S. Behrends,⁽²⁾ S. Belforte,⁽¹⁷⁾ G. Bellettini,⁽¹⁷⁾ J. Bellinger,⁽²⁵⁾
D. Benjamin,⁽²⁴⁾ J. Benlloch,^(6,a) J. Bensinger,⁽²⁾ A. Beretvas,⁽⁶⁾ J. P. Berge,⁽⁶⁾
S. Bertolucci,⁽⁷⁾ K. Biery,^(16,a) S. Bhadra,⁽⁹⁾ M. Binkley,⁽⁶⁾ D. Bisello,⁽¹⁵⁾ R. Blair,⁽¹⁾
C. Blocker,⁽²⁾ A. Bodek,⁽¹⁹⁾ V. Bolognesi,⁽¹⁷⁾ A. W. Booth,⁽⁶⁾ C. Boswell,⁽¹⁰⁾
G. Brandenburg,⁽⁸⁾ D. Brown,⁽⁸⁾ E. Buckley-Geer,⁽²¹⁾ H. S. Budd,⁽¹⁹⁾ G. Busetto,⁽¹⁵⁾
A. Byon-Wagner,⁽⁶⁾ K. L. Byrum,⁽²⁵⁾ C. Campagnari,⁽⁶⁾ M. Campbell,⁽¹⁴⁾ A. Caner,⁽⁶⁾
R. Carey,⁽⁸⁾ W. Carithers,⁽¹²⁾ D. Carlsmith,⁽²⁵⁾ J. T. Carroll,⁽⁶⁾ R. Cashmore,^(6,a)
A. Castro,⁽¹⁵⁾ F. Cervelli,⁽¹⁷⁾ K. Chadwick,⁽⁶⁾ J. Chapman,⁽¹⁴⁾ G. Chiarelli,⁽⁷⁾
W. Chinowsky,⁽¹²⁾ S. Cihangir,⁽⁶⁾ A. G. Clark,⁽⁶⁾ M. Cobal,⁽¹⁷⁾ D. Connor,⁽¹⁶⁾
M. Contreras,⁽⁴⁾ J. Cooper,⁽⁶⁾ M. Cordelli,⁽⁷⁾ D. Crane,⁽⁶⁾ J. D. Cunningham,⁽²⁾
C. Day,⁽⁶⁾ F. DeJongh,⁽⁶⁾ S. Dell'Agnello,⁽¹⁷⁾ M. Dell'Orso,⁽¹⁷⁾ L. Demortier,⁽²⁰⁾
B. Denby,⁽⁶⁾ P. F. Derwent,⁽¹⁴⁾ T. Devlin,⁽²¹⁾ D. DiBitonto,⁽²²⁾ M. Dickson,⁽²⁰⁾
R. B. Drucker,⁽¹²⁾ K. Einsweiler,⁽¹²⁾ J. E. Elias,⁽⁶⁾ R. Ely,⁽¹²⁾ S. Eno,⁽⁴⁾
S. Errede,⁽⁹⁾ A. Etchegoyen,^(6,a) B. Farhat,⁽¹³⁾ G. J. Feldman,⁽⁸⁾ B. Flaughner,⁽⁶⁾
Submitted to Physical Review Letters, December 21, 1992.

G. W. Foster,⁽⁶⁾ M. Franklin,⁽⁸⁾ J. Freeman,⁽⁶⁾ H. Frisch,⁽⁴⁾ T. Fuess,⁽⁶⁾ Y. Fukui,⁽¹¹⁾
 A. F. Garfinkel,⁽¹⁸⁾ A. Gauthier,⁽⁹⁾ S. Geer,⁽⁶⁾ D. W. Gerdes,⁽⁴⁾ P. Giannetti,⁽¹⁷⁾
 N. Giokaris,⁽²⁰⁾ P. Giromini,⁽⁷⁾ L. Gladney,⁽¹⁶⁾ M. Gold,⁽¹²⁾ J. Gonzalez,⁽¹⁶⁾
 K. Goulianos,⁽²⁰⁾ H. Grassmann,⁽¹⁵⁾ G. M. Grieco,⁽¹⁷⁾ R. Grindley,^(16,a) C. Grosso-
 Pilcher,⁽⁴⁾ C. Haber,⁽¹²⁾ S. R. Hahn,⁽⁶⁾ R. Handler,⁽²⁵⁾ K. Hara,⁽²³⁾ B. Harral,⁽¹⁶⁾
 R. M. Harris,⁽⁶⁾ S. A. Hauger,⁽⁵⁾ J. Hauser,⁽³⁾ C. Hawk,⁽²¹⁾ T. Hessing,⁽²²⁾
 R. Hollebeek,⁽¹⁶⁾ L. Holloway,⁽⁹⁾ S. Hong,⁽¹⁴⁾ G. Houk,⁽¹⁶⁾ P. Hu,⁽²¹⁾ B. Hubbard,⁽¹²⁾
 B. T. Huffman,⁽¹⁸⁾ R. Hughes,⁽¹⁶⁾ P. Hurst,⁽⁸⁾ J. Huth,⁽⁶⁾ J. Hysten,⁽⁶⁾ M. Incagli,⁽¹⁷⁾
 T. Ino,⁽²³⁾ H. Iso,⁽²³⁾ H. Jensen,⁽⁶⁾ C. P. Jessop,⁽⁸⁾ R. P. Johnson,⁽⁶⁾ U. Joshi,⁽⁶⁾
 R. W. Kadel,⁽¹²⁾ T. Kamon,⁽²²⁾ S. Kanda,⁽²³⁾ D. A. Kardelis,⁽⁹⁾ I. Karliner,⁽⁹⁾
 E. Kearns,⁽⁸⁾ L. Keeble,⁽²²⁾ R. Kephart,⁽⁶⁾ P. Kesten,⁽²⁾ R. M. Keup,⁽⁹⁾ H. Keutelian,⁽⁶⁾
 D. Kim,⁽⁶⁾ S. B. Kim,⁽¹⁴⁾ S. H. Kim,⁽²³⁾ Y. K. Kim,⁽¹²⁾ L. Kirsch,⁽²⁾ K. Kondo,⁽²³⁾
 J. Konigsberg,⁽⁸⁾ K. Kordas,^(16,a) E. Kovacs,⁽⁶⁾ M. Krasberg,⁽¹⁴⁾ S. E. Kuhlmann,⁽¹⁾
 E. Kuns,⁽²¹⁾ A. T. Laasanen,⁽¹⁸⁾ S. Lammel,⁽³⁾ J. I. Lamoureux,⁽²⁵⁾ S. Leone,⁽¹⁷⁾
 J. D. Lewis,⁽⁶⁾ W. Li,⁽¹⁾ P. Limon,⁽⁶⁾ M. Lindgren,⁽³⁾ T. M. Liss,⁽⁹⁾ N. Lockyer,⁽¹⁶⁾
 M. Loreti,⁽¹⁵⁾ E. H. Low,⁽¹⁶⁾ D. Lucchesi,⁽¹⁷⁾ C. B. Luchini,⁽⁹⁾ P. Lukens,⁽⁶⁾
 P. Maas,⁽²⁵⁾ K. Maeshima,⁽⁶⁾ M. Mangano,⁽¹⁷⁾ J. P. Marriner,⁽⁶⁾ M. Mariotti,⁽¹⁷⁾
 R. Markeloff,⁽²⁵⁾ L. A. Markosky,⁽²⁵⁾ R. Mattingly,⁽²⁾ P. McIntyre,⁽²²⁾ A. Menzione,⁽¹⁷⁾
 E. Meschi,⁽¹⁷⁾ T. Meyer,⁽²²⁾ S. Mikamo,⁽¹¹⁾ M. Miller,⁽⁴⁾ T. Mimashi,⁽²³⁾ S. Miscetti,⁽⁷⁾
 M. Mishina,⁽¹¹⁾ S. Miyashita,⁽²³⁾ Y. Morita,⁽²³⁾ S. Moulding,⁽²⁾ J. Mueller,⁽²¹⁾
 A. Mukherjee,⁽⁶⁾ T. Muller,⁽³⁾ L. F. Naka,⁽²⁾ I. Nakano,⁽²³⁾ C. Nelson,⁽⁶⁾
 D. Neuberger,⁽³⁾ C. Newman-Holmes,⁽⁶⁾ J. S. T. Ng,⁽⁸⁾ M. Ninomiya,⁽²³⁾

L. Nodulman,⁽¹⁾ S. Ogawa,⁽²³⁾ R. Paoletti,⁽¹⁷⁾ V. Papadimitriou,⁽⁶⁾ A. Para,⁽⁶⁾
E. Pare,⁽⁸⁾ S. Park,⁽⁶⁾ J. Patrick,⁽⁶⁾ G. Pauletta,⁽¹⁷⁾ L. Pescara,⁽¹⁵⁾ T. J. Phillips,⁽⁵⁾
F. Ptohos,⁽⁸⁾ R. Plunkett,⁽⁶⁾ L. Pondrom,⁽²⁵⁾ J. Proudfoot,⁽¹⁾ G. Punzi,⁽¹⁷⁾
D. Quarrie,⁽⁶⁾ K. Ragan,^(16,a) G. Redlinger,⁽⁴⁾ J. Rhoades,⁽²⁵⁾ M. Roach,⁽²⁴⁾
F. Rimondi,^(6,a) L. Ristori,⁽¹⁷⁾ W. J. Robertson,⁽⁵⁾ T. Rodrigo,⁽⁶⁾ T. Rohaly,⁽¹⁶⁾
A. Roodman,⁽⁴⁾ W. K. Sakumoto,⁽¹⁹⁾ A. Sansoni,⁽⁷⁾ R. D. Sard,⁽⁹⁾ A. Savoy-
Navarro,⁽⁶⁾ V. Scarpine,⁽⁹⁾ P. Schlabach,⁽⁸⁾ E. E. Schmidt,⁽⁶⁾ O. Schneider,⁽¹²⁾
M. H. Schub,⁽¹⁸⁾ R. Schwitters,⁽⁸⁾ A. Scribano,⁽¹⁷⁾ S. Segler,⁽⁶⁾ Y. Seiya,⁽²³⁾
G. Sganos,^(16,a) M. Shapiro,⁽¹²⁾ N. M. Shaw,⁽¹⁸⁾ M. Sheaff,⁽²⁵⁾ M. Shochet,⁽⁴⁾
J. Siegrist,⁽¹²⁾ A. Sill,⁽¹⁹⁾ P. Sinervo,^(16,a) J. Skarha,⁽¹⁰⁾ K. Sliwa,⁽²⁴⁾ D. A. Smith,⁽¹⁷⁾
F. D. Snider,⁽¹⁰⁾ L. Song,⁽⁶⁾ T. Song,⁽¹⁴⁾ M. Spahn,⁽¹²⁾ A. Spies,⁽¹⁰⁾ P. Sphicas,⁽¹³⁾
R. St. Denis,⁽⁸⁾ L. Stanco,^(6,a) A. Stefanini,⁽¹⁷⁾ G. Sullivan,⁽⁴⁾ K. Sumorok,⁽¹³⁾
R. L. Swartz, Jr.,⁽⁹⁾ M. Takano,⁽²³⁾ K. Takikawa,⁽²³⁾ S. Tarem,⁽²⁾ F. Tartarelli,⁽¹⁷⁾
S. Tether,⁽¹³⁾ D. Theriot,⁽⁶⁾ M. Timko,⁽²⁴⁾ P. Tipton,⁽¹⁹⁾ S. Tkaczyk,⁽⁶⁾ A. Tollestrup,⁽⁶⁾
J. Tonnison,⁽¹⁸⁾ W. Trischuk,⁽⁸⁾ Y. Tsay,⁽⁴⁾ J. Tseng,⁽¹⁰⁾ N. Turini,⁽¹⁷⁾ F. Ukegawa,⁽²³⁾
D. Underwood,⁽¹⁾ S. Vejck, III,⁽¹⁰⁾ R. Vidal,⁽⁶⁾ R. G. Wagner,⁽¹⁾ R. L. Wagner,⁽⁶⁾
N. Wainer,⁽⁶⁾ R. C. Walker,⁽¹⁹⁾ J. Walsh,⁽¹⁶⁾ G. Watts,⁽¹⁹⁾ T. Watts,⁽²¹⁾ R. Webb,⁽²²⁾
C. Wendt,⁽²⁵⁾ H. Wenzel,⁽¹⁷⁾ W. C. Wester, III,⁽¹²⁾ T. Westhusing,⁽⁹⁾ S. N. White,⁽²⁰⁾
A. B. Wicklund,⁽¹⁾ E. Wicklund,⁽⁶⁾ H. H. Williams,⁽¹⁶⁾ B. L. Winer,⁽¹⁹⁾ J. Wolinski,⁽²²⁾
D. Y. Wu,⁽¹⁴⁾ J. Wyss,⁽¹⁵⁾ A. Yagil,⁽⁶⁾ K. Yasuoka,⁽²³⁾ Y. Ye,^(16,a) G. P. Yeh,⁽⁶⁾
C. Yi,⁽¹⁶⁾ J. Yoh,⁽⁶⁾ M. Yokoyama,⁽²³⁾ J. C. Yun,⁽⁶⁾ A. Zanetti,⁽¹⁷⁾ F. Zetti,⁽¹⁷⁾
S. Zhang,⁽¹⁴⁾ W. Zhang,⁽¹⁶⁾ S. Zucchelli,^(6,a)

The CDF Collaboration

- (1) *Argonne National Laboratory, Argonne, Illinois 60439*
- (2) *Brandeis University, Waltham, Massachusetts 02254*
- (3) *University of California at Los Angeles, Los Angeles, California 90024*
- (4) *University of Chicago, Chicago, Illinois 60637*
- (5) *Duke University, Durham, North Carolina 27706*
- (6) *Fermi National Accelerator Laboratory, Batavia, Illinois 60510*
- (7) *Laboratori Nazionali di Frascati, Istituto Nazionale di Fisica Nucleare, Frascati, Italy*
- (8) *Harvard University, Cambridge, Massachusetts 02138*
- (9) *University of Illinois, Urbana, Illinois 61801*
- (10) *The Johns Hopkins University, Baltimore, Maryland 21218*
- (11) *National Laboratory for High Energy Physics (KEK), Japan*
- (12) *Lawrence Berkeley Laboratory, Berkeley, California 94720*
- (13) *Massachusetts Institute of Technology, Cambridge, Massachusetts 02139*
- (14) *University of Michigan, Ann Arbor, Michigan 48109*
- (15) *Università di Padova, Istituto Nazionale di Fisica Nucleare, Sezione di Padova, I-35131 Padova, Italy*
- (16) *University of Pennsylvania, Philadelphia, Pennsylvania 19104*
- (17) *Istituto Nazionale di Fisica Nucleare, University and Scuola Normale Superiore of Pisa, I-56100 Pisa, Italy*
- (18) *Purdue University, West Lafayette, Indiana 47907*
- (19) *University of Rochester, Rochester, New York 15627*
- (20) *Rockefeller University, New York, New York 10021*

(21) *Rutgers University, Piscataway, New Jersey 08854*

(22) *Texas A&M University, College Station, Texas 77843*

(23) *University of Tsukuba, Tsukuba, Ibaraki 305, Japan*

(24) *Tufts University, Medford, Massachusetts 02155*

(25) *University of Wisconsin, Madison, Wisconsin 53706*

(a) *Visitor*

Abstract

We present measurements from events with two isolated prompt photons in $\bar{p}p$ collisions at $\sqrt{s} = 1.8$ TeV. The differential cross section, measured as a function of transverse momentum (P_T) of each photon, is about three times what next-to-leading-order QCD calculations predict. The cross section for photons with P_T in the range 10 to 19 GeV is $86 \text{ pb} \pm 27(\text{stat})^{+32}_{-23}(\text{syst})$. We also study the correlation between the two photons in both azimuthal angle and P_T . The magnitude of the vector sum of the transverse momenta of both photons, $K_T = |\vec{P}_{T1} + \vec{P}_{T2}|$, has a mean value of $\langle K_T \rangle = 5.1 \pm 1.1$ GeV.

In this letter we present the first measurements of prompt diphoton production in proton-antiproton collisions at $\sqrt{s} = 1.8$ TeV. Prompt diphotons are two photons produced in the initial collision, in contrast to photons produced by decays of hadrons. According to Quantum Chromodynamics (QCD), there are three types of processes that contribute significantly to diphoton production: the Born process ($q\bar{q} \rightarrow \gamma\gamma$), the box process ($gg \rightarrow \gamma\gamma$), and *bremsstrahlung* processes (e.g. $qg \rightarrow \gamma\gamma q$). In addition to studying QCD, there is substantial interest in understanding production of diphotons when the initial state partons have low fractional momentum x , because it is a background to an intermediate mass Higgs signal ($H \rightarrow \gamma\gamma$) at future hadron colliders. Correlations between the two photons can be used to study K_T , the transverse momentum of the initial state partons participating in the hard collision. Previous diphoton measurements have shown that K_T is significant [1].

A detailed description of the Collider Detector at Fermilab (CDF) may be found in Ref. [2]; the components relevant for this analysis are described briefly here. Scintillator-based electromagnetic (EM) and hadronic (HAD) calorimeters in the central region ($|\eta| < 1.1$) are arranged in projective towers of size $\Delta\eta \times \Delta\phi \approx 0.1 \times 0.26$, where η is the pseudorapidity and ϕ is the azimuthal angle with respect to the proton beam. The central electromagnetic strip chambers (CES) are multiwire proportional chambers embedded inside the central EM calorimeter near shower maximum. An

integrated luminosity of 4.3 pb^{-1} was accumulated with a trigger that required two clusters with EM transverse energy (E_T) greater than 10 GeV each. The trigger efficiency per photon, shown in Fig. 1a, was measured from a sample of electrons with $E_T > 5 \text{ GeV}$. Throughout this article P_T is the component of the photon momentum transverse to the beam direction, and E_T is defined similarly. To reject dijet backgrounds, the trigger required that at least 89% of the transverse energy of the photon be in the EM compartment of the calorimeter.

Photons are detected as energy clusters [3] in the electromagnetic calorimeter with an energy resolution $\sigma_E = (13.5\%/\sqrt{E_T}) \oplus 2\%$, where \oplus indicates addition in quadrature. For the average photon, an EM cluster consists of two adjacent towers. First we required the ratio of HAD E_T to EM E_T in each EM cluster be less than $0.055 + 0.045 \times E[\text{GeV}]/100$, and also that the energy shared across tower boundaries in the EM cluster was consistent with that expected for a single electromagnetic shower [3]. The analysis required there be no charged particle tracks pointing at the EM cluster for each photon. We associated the highest energy CES cluster [4] within the boundaries of the each EM cluster with the photon. Candidate photons with additional CES energy deposits greater than 1 GeV were rejected. Fiducial cuts were imposed to avoid uninstrumented regions at the edges of the CES, and each photon was required to be in the pseudorapidity interval $|\eta| < 0.9$ and have P_T in the range $10 < P_T < 35 \text{ GeV}$. The dominant source of background is high energy π^0 and η mesons, which are typically produced in association with other hadrons. An explicit cut on isolation, defined as the ratio of transverse energy in towers bordering

the cluster to the E_T of the cluster itself, was used to reduce these backgrounds. The isolation of each photon candidate when the other candidate is required to have isolation less than 0.1, shown in Fig. 1b, illustrates that requiring isolation less than 0.1 significantly reduced the background from non-isolated decays of π^0 and η mesons opposite a photon. Also in Fig. 1b, the excess of isolated diphoton candidates above the predictions of a background simulation [5], suggests the presence of true diphotons in the data.

To subtract the background, the CES transverse profile of each photon candidate was fit to the profile of electrons measured in a test beam. The $\tilde{\chi}^2$ of that fit was used to statistically separate the contribution of photons and background. The probability that a true photon has $\tilde{\chi}^2 < 4$ is ϵ_γ , the probability that the background has $\tilde{\chi}^2 < 4$ is ϵ_{π^0} ; these probabilities are P_T dependent and were determined in the single photon analysis [4]. Within the range of photon transverse momentum $10 < P_T < 19$ GeV the background can be subtracted reliably; at higher P_T the background overwhelms the negligible signal.

Each event in the diphoton sample is classified into four cases; (1) both photon candidates fail the $\tilde{\chi}^2$ cut at 4, (2) the leading candidate with the highest P_T fails the $\tilde{\chi}^2$ cut and the next one passes it, (3) the leading candidate passes the $\tilde{\chi}^2$ cut and the next one fails it, and (4) both candidates pass the $\tilde{\chi}^2$ cut. The number of photon candidates in each case can be written as a vector ($\vec{N} = (N_{FF}, N_{FP}, N_{PF}, N_{PP})$) and related to the vector of the number of photons and mesons in diphoton and background events ($\vec{W} = (W_{\pi^0\pi^0}, W_{\pi^0\gamma}, W_{\gamma\pi^0}, W_{\gamma\gamma})$) by the matrix equation $\vec{N} = E\vec{W}$,

where \mathbf{E} is a 4×4 matrix of $\tilde{\chi}^2$ efficiencies. Formally

$$N_{AB} = \sum_{\mu\nu} E_{AB}^{\mu\nu} W_{\mu\nu} \quad (1)$$

where A and B each can be either P (passes cut) or F (fails cut), μ and ν each can be either γ (signal) or π^0 (background). The efficiency matrix element $E_{AB}^{\mu\nu}$ is the product of probabilities of producing outcomes A and B from initial states μ and ν , $E_{AB}^{\mu\nu} = P(\mu \rightarrow A)P(\nu \rightarrow B)$, where $P(\mu \rightarrow A) = \epsilon_\mu$ if $A = P$ (passes cut), and $P(\mu \rightarrow A) = (1 - \epsilon_\mu)$ if $A = F$ (fails cut). For example $E_{PF}^{\gamma\pi^0} = \epsilon_\gamma(1 - \epsilon_{\pi^0})$ is the joint probability of a photon passing and a background particle failing. Hence, the elements of \mathbf{E} are simple functions of the two efficiencies ϵ_γ and ϵ_{π^0} .

Inverting equation 1 we obtain the raw number of photons in diphoton events, $W_{\gamma\gamma}$, presented in table I. We correct for acceptance (A) and event selection efficiency (ϵ) to obtain the true number of photons in diphoton events: $N_{\gamma\gamma} = W_{\gamma\gamma}/A\epsilon$. Here A and ϵ account for both photons: $A = A(1)A(2)$ and $\epsilon = \epsilon(1)\epsilon(2)$. The acceptance A , which came from the fiducial cuts alone, was 66% per photon giving 43% per diphoton event. The event selection efficiency is the product of the trigger efficiency (shown in Fig. 1a), the extra cluster cut efficiency (96% at 10 GeV falling to 93% at 20 GeV per photon), and the isolation cut efficiency in the presence of an underlying event (> 90% per photon). The diphoton cross section, which is the differential cross section for finding a photon in a bin of P_T in a diphoton event in which both photons have $P_T > 10$ GeV, is simply given by $d\sigma/dP_T = N_{\gamma\gamma}/(\mathcal{L}\Delta P_T)$, where \mathcal{L} is the luminosity and ΔP_T is the bin width. The diphoton cross section is given in table II and Fig. 2.

In Fig. 2, and in subsequent figures, the inner error bars are statistical and the outer error bars are the statistical and systematic uncertainties added in quadrature. Sources of systematic uncertainty (u) include the trigger efficiency ($1\% < u < 10\%$), the isolation cut efficiency in the presence of an underlying event ($9\% < u < 19\%$), and the background subtraction ($12\% < u < 42\%$).

In Fig. 2 we compare the diphoton differential cross section to the predictions of a QCD calculation [6] to order $\alpha^2\alpha_s$, which includes lowest order Born, box and *bremsstrahlung* processes and most next-to-lowest-order (NLO) processes. The CDF diphoton cross section is roughly three times what the NLO QCD calculation predicts, similar to CDF single photons [4] at low P_T , and the UA2 measurement [7] of diphotons at 11 GeV. Also shown is an analytic calculation of the Born + box processes alone [6], and for comparison the calculation is repeated using the Monte Carlo program PYTHIA [5] with and without *bremsstrahlung*. All calculations include the isolation cut and use HMRSB parton distributions [8]; when MRSD0 parton distributions [9] are used the NLO cross section increases by roughly 20%. The renormalization scale was $\mu^2 = (P_{T1}^2 + P_{T2}^2)/2$ for the analytic calculation, and $\mu^2 = \hat{s}/4$ for PYTHIA because the first scale was not available in PYTHIA. The NLO cross section decreases by less than 6% when μ^2 is increased or decreased by a factor of 10. The differences between the Born + box analytic calculation and PYTHIA are primarily due to K_T effects, discussed in the next paragraph. Calculations that only include the Born and box diagrams, which are commonly used to estimate the prompt diphoton background to Higgs decay at future hadron colliders, are too low by roughly a factor

of five.

We now use diphotons to study the P_T of the initial state partons. Correlations between the two photons in azimuthal angle and P_T can be related directly to the kinematics of the initial state. In Fig. 3 we present measurements of the correlation between the two photons compared with the predictions of PYTHIA using the Born and box diagrams only; including final state photon *bremsstrahlung* processes in the PYTHIA calculation does not significantly change these predictions. The three variables shown are the vector sum of the transverse momenta $K_T = |\vec{P}_{T1} + \vec{P}_{T2}|$, the P_T balance $B = P_{T2}/P_{T1}$, and the azimuthal angular separation $\Delta\phi = \phi_2 - \phi_1$. All of the measurements agree with the PYTHIA calculation which effectively sums up multiple gluon *bremsstrahlung* in the initial state. However, analytic QCD calculations [6] to order $\alpha^2\alpha_s$, do not include multiple gluon *bremsstrahlung*. Unfortunately, this may reduce the precision of analytic calculations, because the correlation variables show that the transverse momentum of initial state partons can significantly affect the final state even for $P_T > 10$ GeV. The mean value of K_T is quite large, $\langle K_T \rangle = 5.1 \pm 1.1$ GeV is the mean of the data in Fig. 3a, and Fig. 4 shows that $\langle K_T \rangle$ is larger at CDF than in previous measurements at lower \sqrt{s} . This may be due to a dependence on other dynamical variables like P_T ; larger event samples that cover higher P_T values should see a larger $\langle K_T \rangle$. Significant K_T , which is often not adequately included in QCD calculations, can affect P_T distributions in hadronic collisions.

In summary, we have measured the diphoton cross section to be $86 \text{ pb} \pm 27(\text{stat})$
 $^{+32}_{-23}$ (syst), for photons with P_T in the range 10 to 19 GeV in events containing two
isolated photons with pseudorapidity $|\eta| < 0.9$. We have measured the mean trans-
verse momentum of the diphoton system to be $\langle K_T \rangle = 5.1 \pm 1.1 \text{ GeV}$. The diphoton
differential cross section is roughly three times what QCD calculations predict, and
may be a larger background to Higgs detection than was previously anticipated.

We thank the Fermilab staff and the technical staffs of the participating institu-
tions for their vital contributions. This work was supported by the U.S. Department of
Energy and National Science Foundation, the Italian Istituto Nazionale di Fisica Nu-
cleare, the Ministry of Science, Culture and Education of Japan, the Natural Sciences
and Engineering Research Council of Canada, and the Alfred P. Sloan Foundation.
We also wish to thank B. Bailey, J. F. Owens, and J. Ohnemus for the results of their
calculation.

References

- [1] E. Bonvin et al., *Phys. Lett.* **B236**(1990)523.
- [2] F. Abe et al., *Nucl. Inst. and Meth.* **A271**(1988)387.
- [3] F. Abe et al., *Phys. Rev.* **D43**(1991)2070.
- [4] F. Abe et al., *Phys. Rev. Lett.* **68**(1992)2734 and F. Abe et al., “A Prompt Photon
Cross Section Measurement in $\bar{p}p$ Collisions at $\sqrt{s} = 1.8 \text{ TeV}$ ”, Fermilab-PUB-

92/01-E, 1992 (to be published).

- [5] PYTHIA 5.4 described in H. Bengtsson and T. Sjostrand, *Comput. Phys. Commun.* **46**(1987)43 was used to generate events which we passed through a detector simulation when necessary.
- [6] B. Bailey, J. F. Owens and J. Ohnemus, *Phys. Rev.* **D46**(1992)2018.
- [7] J. Alitti et. al. (UA2 Collaboration), *Phys. Lett.* **B288**(1992)386.
- [8] Set *B* with $\Lambda_{\overline{MS}} = 190$ MeV in P. N. Harriman et. al., *Phys. Rev.* **D42**(1990)798.
- [9] Set *D0* in A. D. Martin et. al., DTP/92-16, April 1992.
- [10] The K_T was calculated from the data in C. Albajar et al. (UA1 Collaboration), *Phys. Lett.* **B209**(1988)385.
- [11] D. Antreasyan et. al., *Phys. Rev. Lett.* **47**(1981)12.

Table I: For each bin of photon candidate P_T , we list the number of photon candidates contributing to the diphoton $\bar{\chi}^2$ results Fail-Fail (N_{FF}), Fail-Pass + Pass-Fail ($N_{FP}+N_{PF}$), and Pass-Pass (N_{PP}). We also list the results after matrix inversion for the raw number of photons in diphoton events ($W_{\gamma\gamma}$), and photons plus mesons in background events ($W_{\pi^0\pi^0}$ and $W_{\pi^0\gamma} + W_{\gamma\pi^0}$). The first uncertainty on $W_{\gamma\gamma}$ is statistical and the second is systematic.

P_T Bin (GeV/c)	N_{FF}	N_{FP} N_{PF}	N_{PP}	$W_{\pi^0\pi^0}$	$W_{\pi^0\gamma}$ $W_{\gamma\pi^0}$	$W_{\gamma\gamma}$
10-12	14	30	23	34	11	$22 \pm 12 \begin{smallmatrix} +5 \\ -3 \end{smallmatrix}$
12-15	18	49	45	33	35	$44 \pm 20 \begin{smallmatrix} +19 \\ -14 \end{smallmatrix}$
15-19	14	33	27	32	15	$27 \pm 18 \begin{smallmatrix} +11 \\ -8 \end{smallmatrix}$

Table II: For each bin of single photon P_T , we give the mean P_T , the diphoton differential cross section, and its statistical and systematic uncertainties. Each photon was counted once, so that multiplying by the luminosity, bin width, and acceptance gives the number of photons in these diphoton events.

P_T Bin (GeV/c)	Mean P_T (GeV/c)	$d\sigma/dP_T$ [pb/(GeV/c)]	Stat. (%)	Systematic (%)	
10-12	11.1	17.5	57	+31	-21
12-15	13.5	11.6	46	+45	-35
15-19	17.4	4.2	65	+41	-29
10-19	13.3	9.6	31	+37	-27

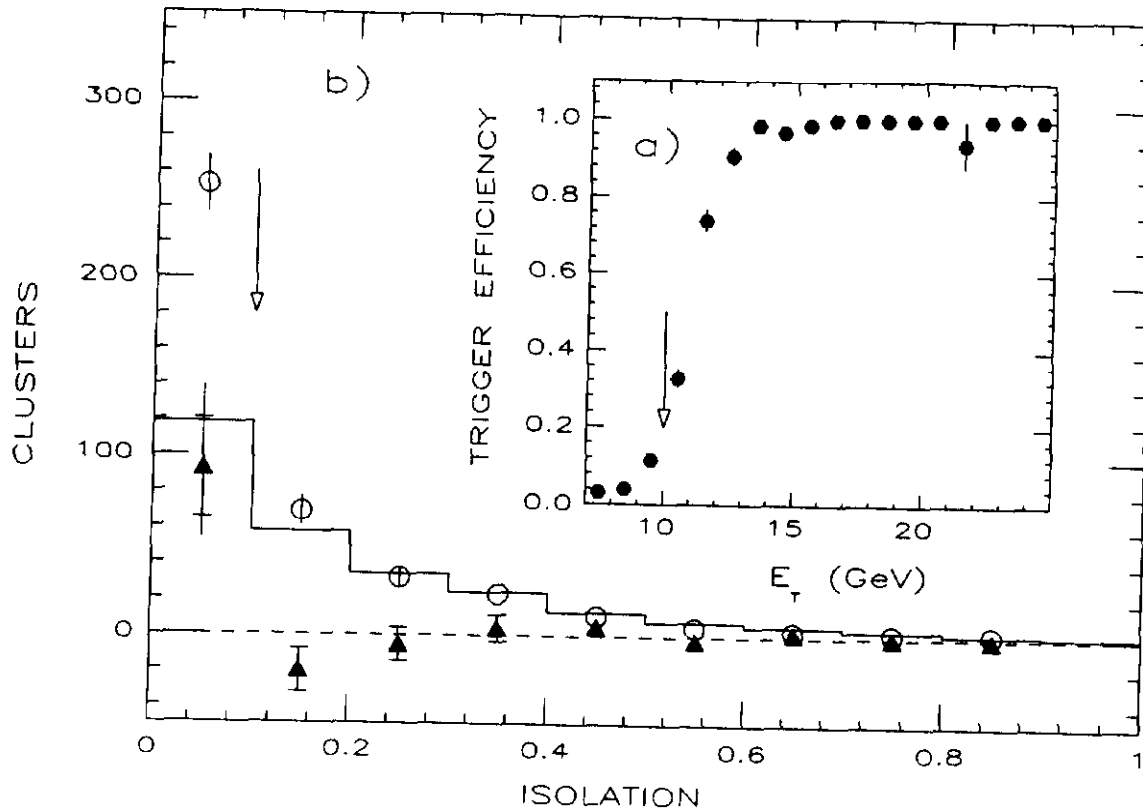


Figure 1: a) The efficiency per photon of the diphoton trigger as a function of photon transverse energy, measured using electrons from a lower threshold trigger. The arrow indicates the smallest photon P_T considered in subsequent analysis. b) The number of neutral EM clusters (open circles) as a function of isolation compared to a simulation (solid histogram) of η and π^0 mesons in jets opposite a photon, normalized to the data to the right of the arrow (predominantly background). The photons (triangles) after background subtraction are almost exclusively to the left of the arrow.

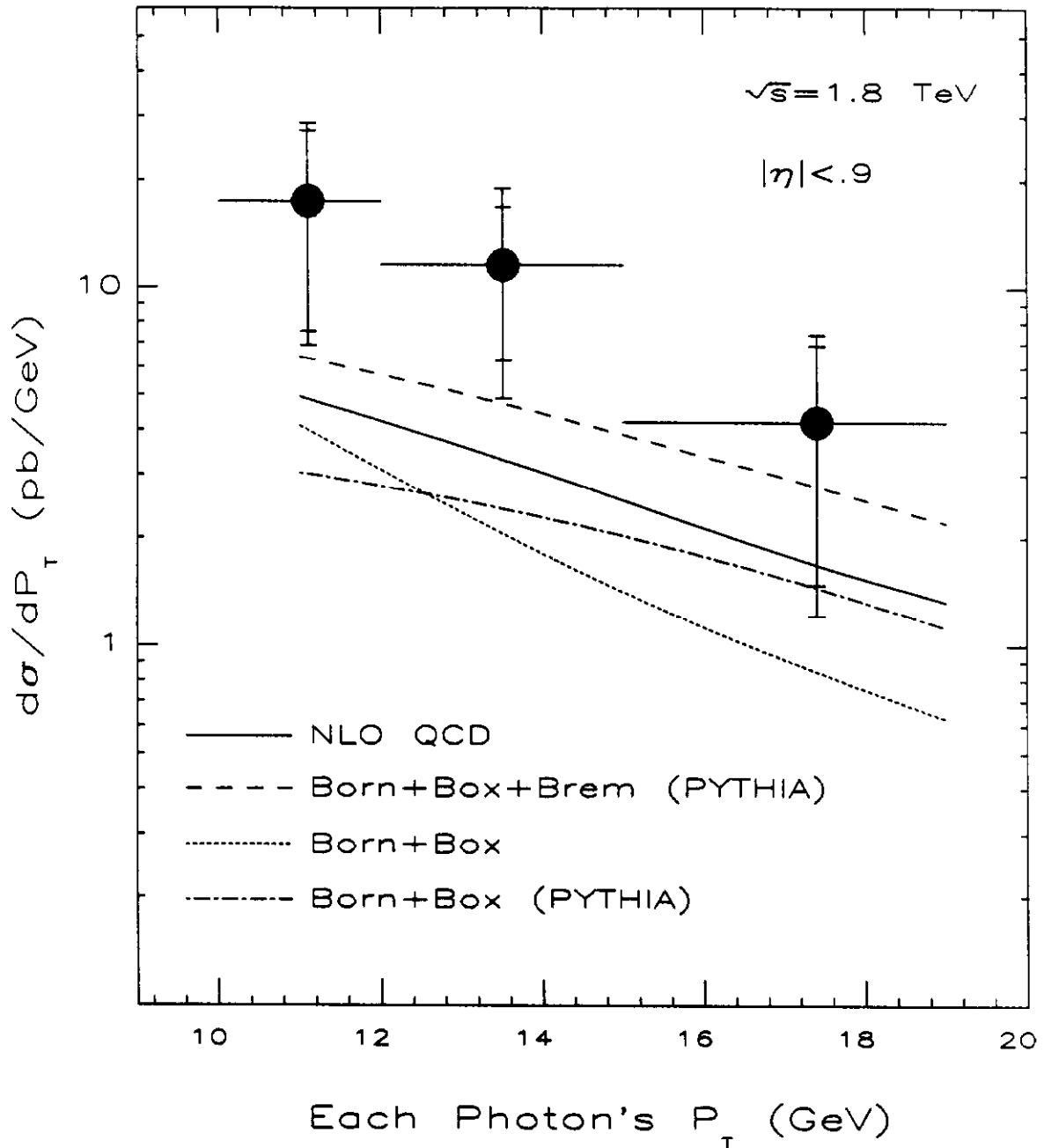


Figure 2: The diphoton differential cross section as a function of the P_T of each photon is compared to analytic QCD predictions [6] at next-to-lowest-order (solid) and lowest order (dots). Monte Carlo calculations using PYTHIA are shown at lowest order with *bremsstrahlung* (dashed) and without (dot-dash).

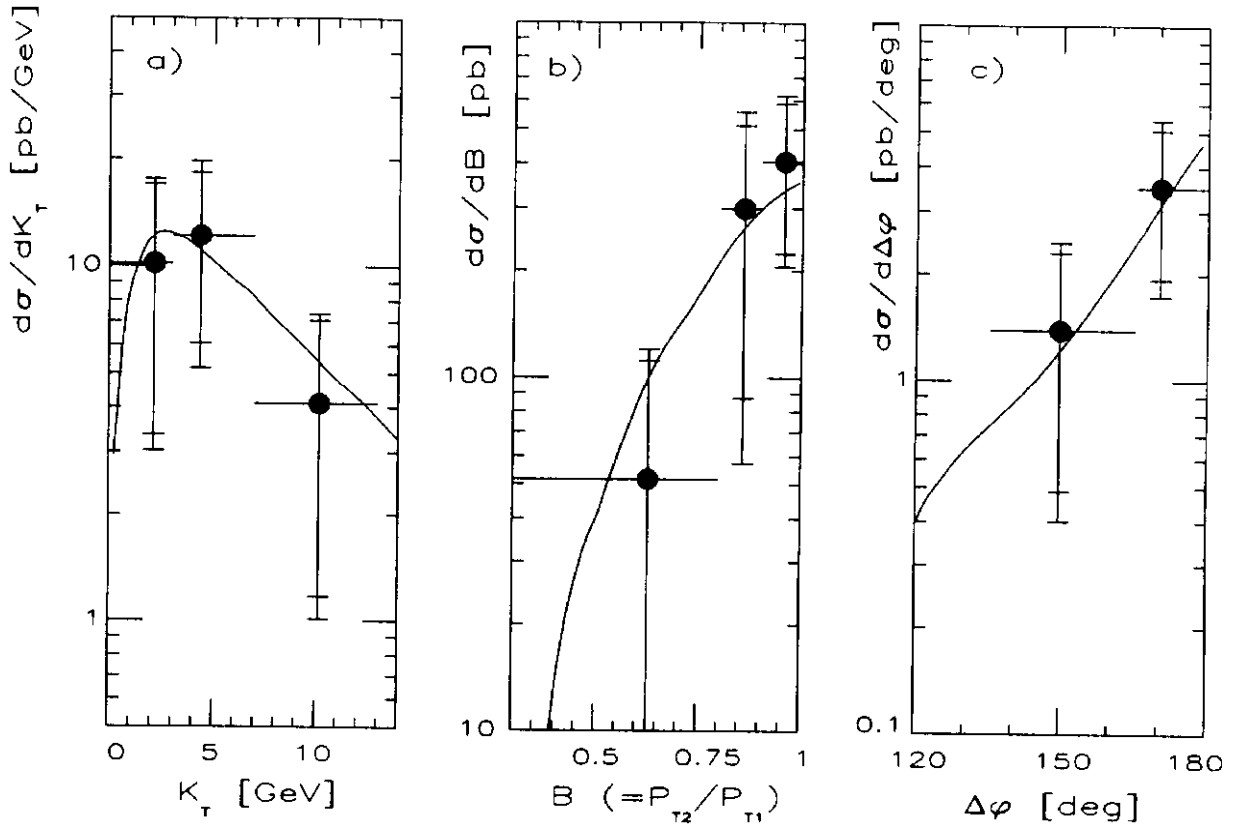


Figure 3: The correlation of the two photons is shown by the cross section versus a) the vector sum of the transverse momenta $K_T = |\vec{P}_{T1} + \vec{P}_{T2}|$, b) the P_T balance $B = P_{T2}/P_{T1}$, and c) the azimuthal angular separation $\Delta\phi = \phi_2 - \phi_1$. Our measurement is compared with a Monte Carlo prediction normalized to the data.

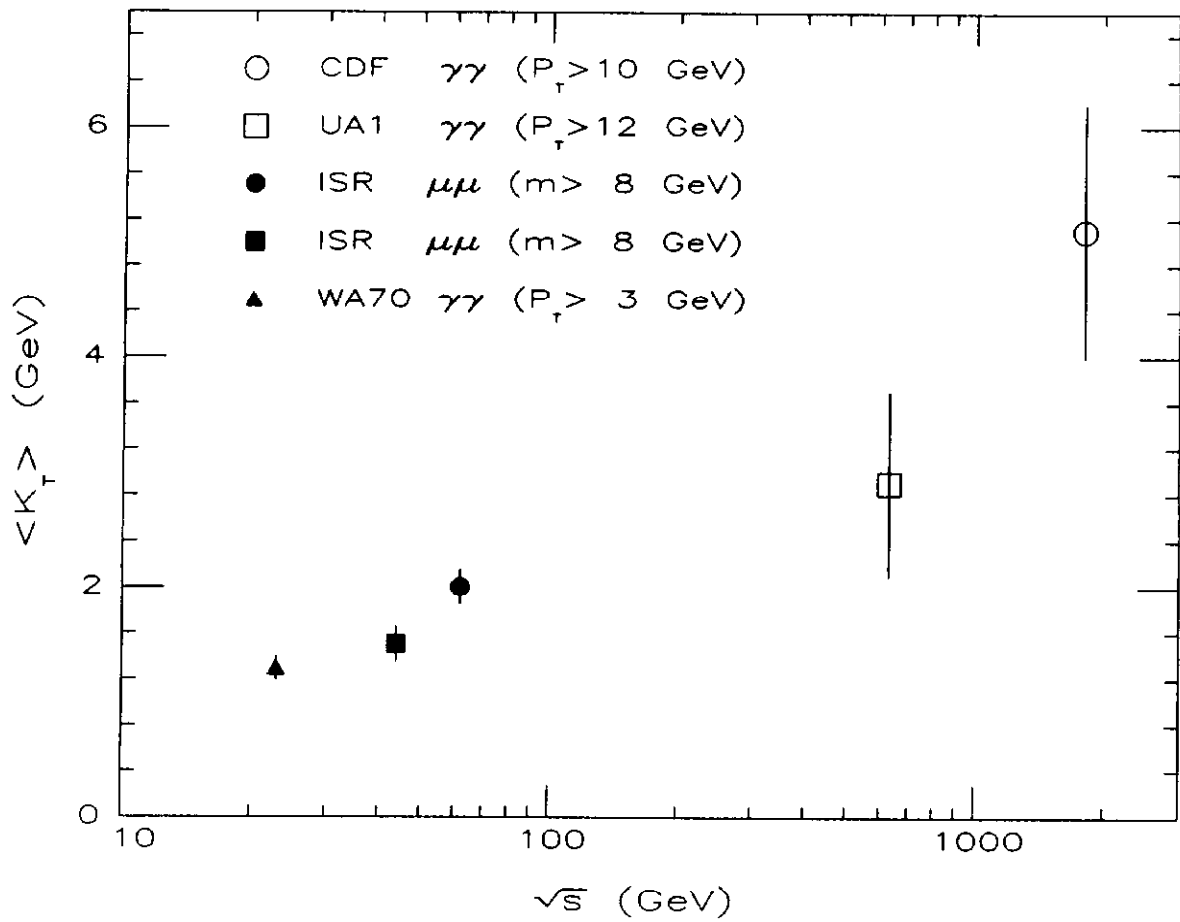


Figure 4: The mean value of K_T versus collision energy measured in diphoton events at CDF, UA1 [10] and WA70 [1] and in high mass dimuon events at the ISR [11].